

# Simulating Bragg Diffraction to Understand Divergence from Theory in an Introductory Laboratory Experiment

Evan Heidtmann

(Dated: 7 May 2008)

Macroscopic Bragg diffraction is an experiment frequently performed at the undergraduate level to prepare students for the more abstract task of analyzing atomic crystals using X-ray scattering. However, the details of the experiment used at the College of Wooster frequently lead to frustration and confusion due to noise and unexplained peaks in the measured data. Here I construct a computer simulation of Bragg scattering off a small crystal and use it to shed some light on the problem.

## I. BACKGROUND AND INTRODUCTION

In 1912, William Henry Bragg and William Lawrence Bragg used X-rays to analyze the structure of atomic crystals. By measuring the X-ray reflections from the crystal at a range of angles, they were able to arrive at an estimate for the average separation between atoms in the crystal and earn a Nobel Prize in 1915 [1].

An analogous experiment is often performed in introductory physics laboratories using microwave radiation and a macroscopic crystal. For example, the Department of Physics at Colorado State University uses a two-dimensional crystal constructed of vertical rods, a polarized microwave source, and a computer data acquisition system to survey the patterns of reflection [2]. At the College of Wooster, students in the sophomore-level Modern Physics course reflect microwaves off small ball bearings embedded in a large Styrofoam block. In both cases, students gain a good intuitive understanding of this method of crystal analysis that can later be applied to microscopic atomic crystals.

However, the experiment here at the College of Wooster is frequently disappointing, for the data obtained usually show a number of different intensity peaks when only two are expected. In addition, the expected peaks often do not coincide well with their expected positions. It is believed that these discrepancies are due to the theoretical assumption that the crystal is of a very large size and that multiple reflections are negligible, but in fact the crystal contains just 125 “atoms” and multiple reflections may be significant. Here I employ a simple computer simulation in an attempt to shed some light on the problem.

## II. THEORETICAL DEVELOPMENT

### A. The Bragg conditions for diffraction

The Braggs conceived of an atomic crystal as an infinite series of planes of atoms, each reflecting some portion of the incident radiation. The observed reflected signal should attain a local maximum amplitude when the reflected waves interfere constructively.

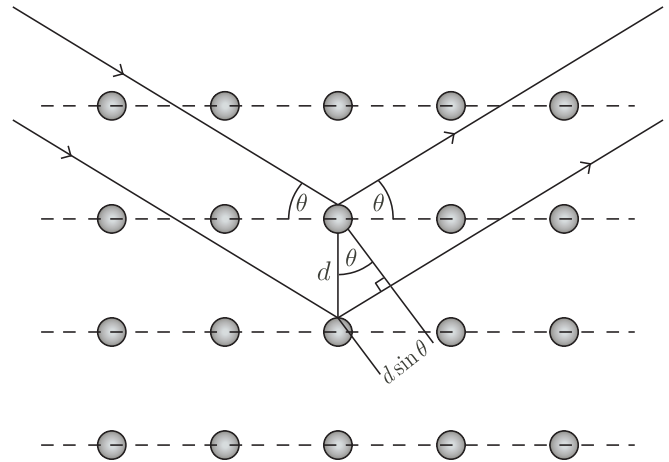


Figure 1: The difference in path length for two rays reflected off adjacent parallel planes of atoms is  $2d \sin \theta$ , where  $d$  is the separation of the planes and  $\theta$  is the angle of incidence (also called the grazing angle).

Now consider two parallel rays reflecting off adjacent crystal planes. We assume that the usual law of reflection applies, so that the angle of incidence is equal to the angle of reflection. If this is the case and if adjacent planes are separated by a distance  $d$  and the rays reflect off adjacent crystal planes, then the additional distance traveled by the ray reflecting off the deeper plane is  $2d \sin \theta$  (See Fig. 1). Constructive interference occurs when this path difference is equal to an integral number of wavelengths, so

$$2d \sin \theta = n\lambda, \quad (1)$$

where  $n$  is an integer. Notice that this requires the wavelength  $\lambda < 2d$  if any constructive interference is to be observed.

If the crystal separation and source wavelength are known, then Eq. 1 can be used to predict the angle  $\theta$  where constructive interference is expected.

### B. Single reflections on a finite crystal

We consider diffraction of electromagnetic radiation off a simple cubic crystal lattice containing  $N^3$  atoms, where  $N$  is a

small integer, usually between 5 and 10. A source is placed at the origin and a detector and crystal are placed elsewhere in space. The source emits a spherical wave in all directions, which is reflected off each of the atoms in the crystal. The observed intensity at the detector is then the vector sum of all such reflected waves.

This model ignores multiple reflections and assumes that the source is properly restricted so that no waves are transmitted directly from source to detector. We also assume that the source emits polarized radiation and that the reflected waves are in approximately the same plane of polarization, so we may treat the radiation as scalar rather than vector waves.

To begin development of the model, recall that a scalar sinusoidal wave due to a spherical source at the origin can be written [3]

$$\mathcal{E}_e[\vec{r}, t] = \frac{\mathcal{E}_1}{r} e^{i(kr - \omega t)}, \quad (2)$$

where

$$r \equiv |\vec{r}| \quad (3)$$

is the magnitude of the position vector locating the point at which the wave is measured and  $\mathcal{E}_1$  is the field amplitude at 1 unit away from the emitter.

Now let  $\vec{a}_{lmn}$  locate an atom in the lattice, where  $l, m, n$  are integers between zero and  $N$ . Then the emitter field at the atom is

$$\mathcal{E}_e[\vec{a}_{lmn}, t] = \frac{\mathcal{E}_1}{a_{lmn}} e^{i(ka_{lmn} - \omega t)}. \quad (4)$$

If the atom reflects the incident wave at some uniform fraction of the amplitude  $f < 1$ , then the field due to the atom  $lmn$  is given by

$$\mathcal{E}_{lmn}[\vec{r}, t] = f \cdot \mathcal{E}_e[\vec{a}_{lmn}, 0] \cdot \frac{e^{i(k|\vec{r} - \vec{a}_{lmn}| - \omega t)}}{|\vec{r} - \vec{a}_{lmn}|} \quad (5)$$

$$= \frac{f \mathcal{E}_1}{a_{lmn} \cdot |\vec{r} - \vec{a}_{lmn}|} e^{i(ka_{lmn} + k|\vec{r} - \vec{a}_{lmn}| - \omega t)}. \quad (6)$$

It follows that the net field observed at the detector located by  $\vec{\mathcal{O}}$  is found by summing these fields over all atoms, so

$$\mathcal{E}_{\mathcal{O}}^{single}[t] \equiv \sum_{l,m,n} \mathcal{E}_{lmn}[\vec{\mathcal{O}}, t] = \sum_{l=0}^N \sum_{m=0}^N \sum_{n=0}^N \mathcal{E}_{lmn}[\vec{\mathcal{O}}, t]. \quad (7)$$

### C. Multiple reflections on a finite crystal

The model in Eq. 7 ignores waves which may reflect off more than one atom in the crystal. If reflection fraction  $f$  is very small, this is a valid approximation. But if  $f$  is not so small, then multiple reflections may be significant. However, the development for this case requires that we abandon the scalar approximation, which is out of the scope of this investigation.

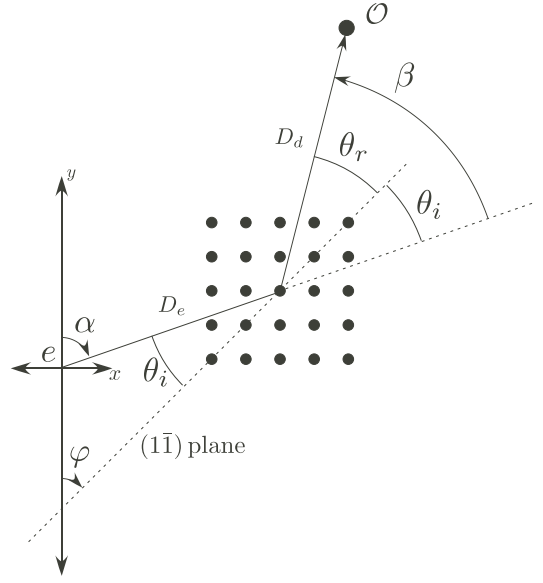


Figure 2: In the computer simulation, the emitter  $e$  is fixed at the origin. The crystal is located by the clockwise angle  $\alpha$  and the distance to the middle  $D_e$ . The observer  $\mathcal{O}$  is located by the counterclockwise angle  $\beta$  and the detector distance  $D_d$ . The angle  $\varphi$  identifies a class of crystal planes; here one  $(\bar{1}\bar{1})$  plane is marked by a dashed line. The relationship between the angle of incidence  $\theta_i$  and the angle of reflection  $\theta_r$  and the parameter angles  $\alpha$  and  $\beta$  can be deduced from the geometry.

### III. GEOMETRY OF THE SIMULATION

The equations in the previous section describe a general situation. To systematically investigate the phenomena of Bragg diffraction, we employ the same geometry as Cornick and Field [2]. The emitter is located at the origin, as shown in Fig. 2. The crystal straddles the  $xy$  plane and its edges parallel the coordinate axes. Thus each atom is located by the vector

$$\vec{a}_{lmn} = d(l\hat{x} + m\hat{y} + n\hat{z}) + \vec{c},$$

where  $\vec{c}$  locates the corner of the crystal nearest the origin,  $d$  is the separation of adjacent atoms, and  $l, m, n$  run from 0 to  $N$ .

The clockwise angle from the vertical  $y$ -axis to the line connecting the emitter with the center of the crystal is labeled  $\alpha$  and the counter-clockwise angle between that same line and the line connecting the crystal center and the detector is labeled  $\beta$ . For all data shown in the next section, the emitter distance  $D_e$  and detector distance  $D_d$  are fixed at 100 times the atom separation and the wavelength  $\lambda$  is fixed at  $4/5$  the atom separation. For a given  $\alpha$  and  $\beta$ , Eq. 7 is evaluated with the aid of a computer to find the field at the observer.

Table I: The expected peak positions may be determined from Eq. 12. This table shows the peaks in  $\alpha$  and  $\beta$  for all values of  $n$ ,  $l$ , and  $k$  which satisfy that equation. All other values result in values for  $\alpha$  and  $\beta$  which are out of range or an argument to the arc sine which is greater than 1. The plane separation  $d_{kl}$  is given as a fraction of atom separation. [2]

$n$	$(kl)$	$d_{kl}$	$\varphi$ (degrees)	$\beta$ (degrees)	$\alpha$ (degrees)
1	(10)	1	0°	47.6°	23.6°
2	(10)	1	0	106.3	53.1
1	(1 $\bar{1}$ )	$\frac{\sqrt{2}}{2}$	45	69.9	79.4
1	(2 $\bar{1}$ )	0.446	$\arctan \frac{1}{2}$	127.5	0.3
1	(2 $\bar{1}$ )	0.446	$-\arctan \frac{1}{2}$	127.5	37.18

#### IV. SIMULATED DATA AND ANALYSIS

##### A. Single reflection

There are many different crystal planes in a cubic lattice. Each is identified by its Miller indices, which are the smallest integers  $(kl)$  such that  $k\hat{x} + l\hat{y}$  is normal to the plane. There are two normals to each plane; we choose the normal that has positive  $x$  component (or, failing that, negative  $y$  component). For example, Fig. 1 depicts reflection off the plane with Miller indices  $(0\bar{1})$ , where  $\bar{1} \equiv -1$ . The plane passing through the main diagonal has Miller indices  $(1\bar{1})$  [2].

As described in Section II A, the Bragg conditions of constructive interference are

$$\theta_i = \theta_r \equiv \theta \quad (8)$$

and

$$2d_{kl} \sin \theta = n\lambda, \quad (9)$$

where  $d_{kl}$  is the perpendicular separation of two adjacent planes with Miller indices  $(kl)$ . Referring to Fig. 2, we see

$$\beta = \theta_i + \theta_r = 2\theta. \quad (10)$$

If we define  $\varphi$  as the clockwise angle the plane makes with the  $y$ -axis, then

$$\theta_i = \theta = \alpha - \varphi. \quad (11)$$

Combining Eqs. 10, 11 and 9, we see

$$\beta = 2 \arcsin \left( \frac{n\lambda}{2d_{kl}} \right), \quad \alpha = \beta/2 + \varphi. \quad (12)$$

From these equations we may compute the positions of the expected peaks in  $\alpha$  and  $\beta$ . Following Cornick and Field, these positions are given in Table I.

Fig. 3 shows a representative intensity plot for a crystal of size  $N = 8$ . All predicted peaks are evident and the peak at  $\alpha = 90^\circ$  wraps around to  $\alpha = 0^\circ$ , so no significant peaks are unexplained. We note that, although the simulated peaks are somewhat broad, they correspond very well with theoretical predictions.

##### B. Multiple reflection

Cornick and Field report that multiple scattering accounts for a net shift in peak position in the direction of positive  $\beta$  [2]. However, the scalar field approximation we employ is not valid for multiple scattering because, within the crystal, the initial polarized field will be oriented in many different directions. Future work to develop a simulation capable of multiple scattering would be very worthwhile.

##### C. Correlation with Modern Physics experiment

The red line in Fig. 3 represents the  $\theta_i = \theta_r$  line measured by students in the Modern Physics course at the College of Wooster. From this plot alone, we see that we expect two large peaks as well as a collection of smaller peaks. Taking the cross-section along that line and re-parameterizing by  $\theta$ , we obtain curves of expected intensity for crystal sizes  $N = 5$  and  $N = 8$ . We may qualitatively compare these curves, in Fig. 4, to an experimental data set shown in Fig. 5 obtained by a team of students in the Modern Physics course. [4]

The experimental curve (Fig. 5) and the simulated curve for  $N = 8$  (Fig. 4) both show major peaks around 20 degrees and 50 degrees and a few smaller peaks nearby. Students performing the experiment usually attribute these smaller peaks to noise, but the simulation shows that they may in fact represent real phenomena. However, there is significant divergence between simulation and experiment for  $N = 5$ . Near 20 degrees, the simulation produces a valley, while experiment shows a peak. This trend was observed in almost all simulated data for  $N \leq 10$ : even  $N$  show all expected peaks, while odd  $N$  show valleys in three of five locations. It is hoped that the future implementation of multiple scattering will eliminate this discrepancy.

#### V. FUTURE WORK AND CONCLUSION

It is clear that any future work on this project should first implement a simulation capable of multiple scattering. In reality multiple scattering probably has a significant effect on the observed data. According to Cornick and Field, multiple scattering is responsible for a net shift in observed peak positions. Multiple scattering may also be able to account for the observed peak in experimental data which appears as a valley in simulations for odd values of  $N$ .

As currently conceived, the implementation of multiple scattering will require that the electric field be represented by a vector. This change in itself will make possible the investigation of different emitter and detector distances. In the Modern Physics experiment, the emitter and detector are separated from the crystal by no more than twice the crystal width, while in the simulation the scalar approximation requires that the

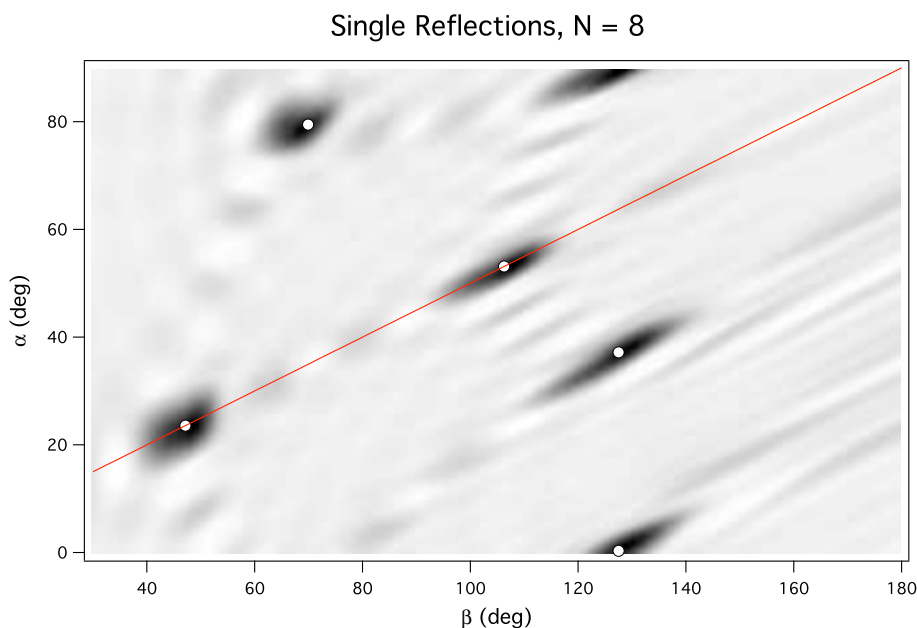


Figure 3: A plot of field intensity versus parameter angles  $\alpha$  and  $\beta$  for crystal size  $N = 8$  shows the peaks of constructive interference in parameter space: darker shades correspond to greater intensities. Here only single reflections were performed. The white dots show the expected peak positions based on the theory due to the Braggs. The red line is the  $\theta_i = \theta_r$  line. One can see that there is good agreement with theory; the plot is also qualitatively very similar to that produced by Cornick and Field [2].

emitter and detector be placed very far from the crystal. A vector-based implementation would allow the simulation to more closely model the physical experiment. If the fine structure observed in Fig. 3 persists under the new simulation, some investigation and explanation of the lesser peaks would be in order.

It may also be useful to incorporate direct transmission from emitter to detector in the simulation. The very large values evident at small  $\theta$  in the experimental plot are believed to be due to spillover from the emitter. Implementation of this effect in the simulation would allow us to estimate the minimum angle  $\theta$  where direction transmission is insignificant.

Despite these shortcomings, the existing simulation is able to

represent the principal components of Bragg scattering. The simulation has also been able to show that some small peaks may be expected in the data measured by Modern Physics students, even when noise is reduced to a minimum.

#### Acknowledgments

I wish to thank Dr. John Lindner for his invaluable help in developing the equations used in the simulation, in interpreting the data, and in locating references.

- 
- [1] Physics 205 Lab Manual. John Lindner, Department of Physics, The College of Wooster.
  - [2] Microwave Bragg diffraction in a model crystal lattice for the undergraduate laboratory. M. T. Cornick and S. B. Field. *Am J. Phys.* 72 (2), February 2004.
  - [3] Weisstein, Eric W.. "Spherical Wave." Eric Weisstein's World of Physics. 2007. Wolfram Research. 6 Mar 2008

<http://scienceworld.wolfram.com/physics/SphericalWave.html>.

- [4] Quantitative comparison is not possible because the experimental data is no longer available in raw form. In addition, the Modern Physics experiment has a wavelength to separation ratio  $\lambda/d \approx 0.74$  while the simulation has  $\lambda/d = 0.8$ .

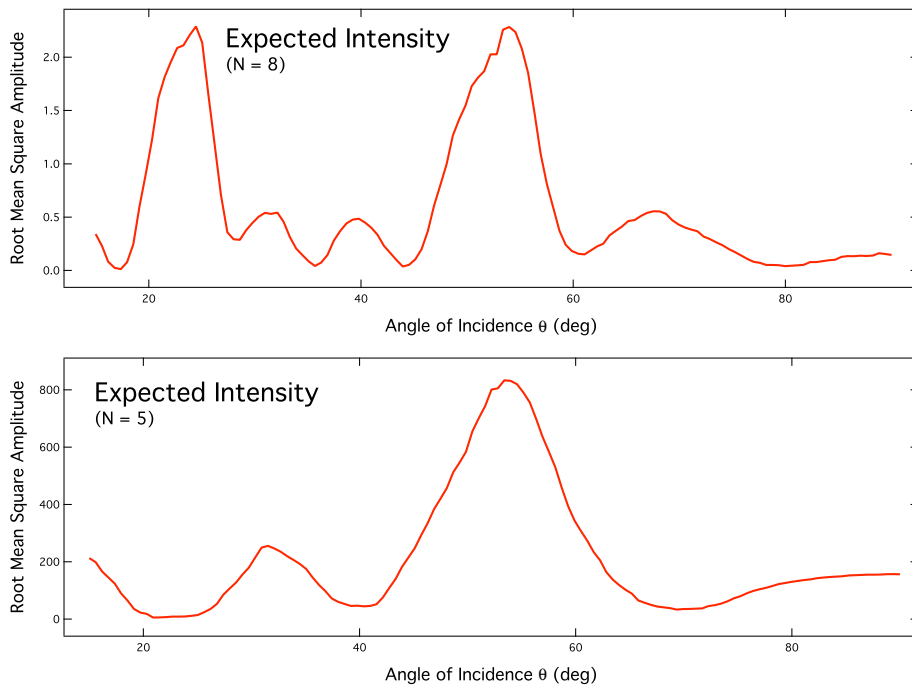


Figure 4: For  $N = 5$  and  $N = 8$ , we show the expected intensity versus angle of incidence for the case  $\theta_i = \theta_r$ .

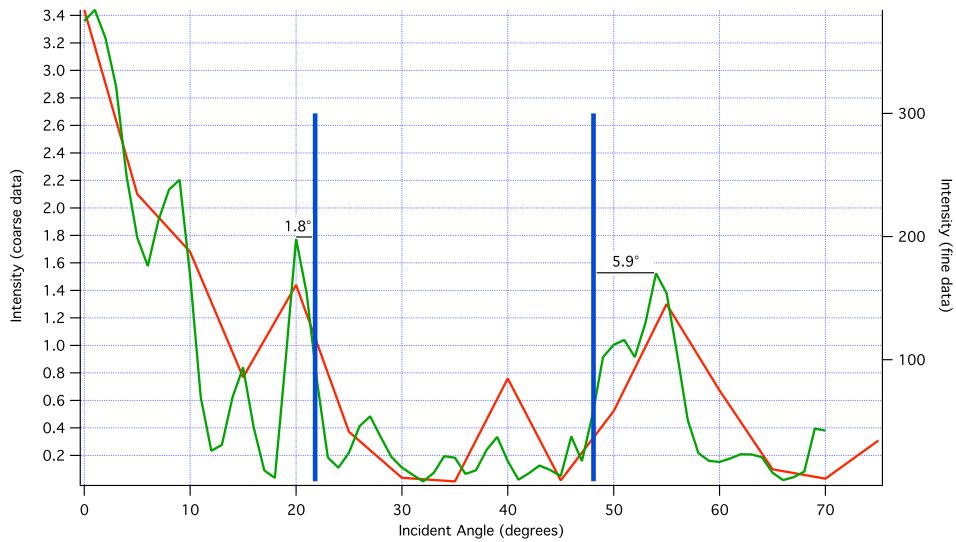


Figure 5: Measured microwave intensity versus grazing angle. Both fine (green) and coarse (red) data sets are shown, as well as the theoretical position of constructive interference peaks in blue. The labeled angles represent the difference in position between the blue line and the green peaks. The data and plot are taken from the 2006 lab report written by Evan Heidtmann and Mike Zappitello.